The luminescence enhancement of Eu^{3+} ion and SnO_2 nanocrystal co-doped sol–gel SiO_2 films*

Zhang Xiao-Wei(张晓伟), Lin Tao(林 涛), Xu Jun(徐 骏)†, Xu Ling(徐 岭), and Chen Kun-Ji(陈坤基)

National Laboratory of Solid State Microstructures, School of Electronic Science and Engineering and School of Physics, Jiangsu Provincial Key Laboratory of Advanced Photonic and Electronic Materials, Nanjing University, Nanjing 210093, *China*

(Received 22 July 2011; revised manuscript received 5 September 2011)

SnO_2 nanocrystal and rare-earth Eu^{3+} ion co-doped SiO_2 thin films are prepared by sol–gel and spin coating methods. The formation of tetragonal rutile structure SnO_2 nanocrystals with a uniform distribution is confirmed by X-ray diffraction and transmission electron microscopy. Fourier transform infrared spectroscopy is used to investigate the densities of the hydroxyl groups, and it is found that the emission intensity from the $^5D_0-^7F_2$ transitions of the Eu^{3+} ions is enhanced by two orders of magnitude due to energy transfer from the oxygen-vacancy-related defects of the SnO_2 nanocrystals to nearby Eu^{3+} ions. The influences of the amounts of Sn and the post-annealing temperatures are systematically evaluated to further understand the mechanism of energy transfer. The luminescence intensity ratio of Eu^{3+} ions from electric dipole transition and magnetic dipole transition indicate the different probable locations of Eu^{3+} ions in the sol–gel thin film, which are further discussed based on temperature-dependent photoluminescence measurements.

Keywords: sol–gel processes, luminescence, rare-earth ions, nanostructured material

PACS: 81.20.Fw, 78.40.Fy, 78.55.–m, 61.46.Hk **DOI:** 10.1088/1674-1056/21/1/018101

1. Introduction

In recent years, rare-earth (RE) elements encapsulated in an SiO_2 matrix have been demonstrated to be promising materials with high luminescence efficiency for a wide range of applications in many kinds of devices.[1−3] SiO_2 is considered a good host matrix for RE ions because of its transparency, compositional variety and ease of production, especially in optical devices.[4] However, owing to forbidden intra-4f transitions, RE ions have very small optical absorption cross sections of the order of 10^{-21} cm^2 in the SiO_2 matrix, which leads to low emission efficiency.[5] Co-doping of semiconductor nanocrystals with large absorption cross sections is an effective way to improve RE luminescence intensity.

More recently, RE ion-doped SiO_2 amorphous matrices containing Si nanocrystals have been reported to evidence the energy transfer from Si nanocrystals to RE ions.[6−8] However, thermal quenching of luminescence, which is a fatal drawback for optical applications, can be ascribed to the reversed energy transfer from RE ions to Si nanocrystals because of the narrow band-gap of the Si semiconductor.[9] In order to eliminate the reversed energy transfer effect, nanocrystals confined in the SiO_2 matrix with a wider band-gap, such as ZnO[10,11] and In_2O_3,[12−14] have been used to replace Si nanocrystals. Therefore, it is necessary to select appropriate nanoparticles as sensitizers in the SiO_2 matrix. SnO_2 nanocrystals, which are cheap and non-toxic, present a wide band-gap of 3.6 eV at 300 K and good spectral overlapping with excitation of Eu^{3+} ions in the emission spectra. Due to the suitable size and density even at the annealing temperature of above 1400 °C, SnO_2 nanocrystals have been theoretically proven to be appropriate sensitizers in Eu^{3+} ion-doped SiO_2 thin films. Moreover, the emission of Eu^{3+} ions is easily observed in visible light, which can be attributed to the $^5D_0-^7F_{j(0-4)}$ transitions. It was indicated previously that Eu^{3+} ions doped into or co-doped with SnO_2 nanocrystals showed special emission peaks, mainly ascribed to the magnetic dipole transition of Eu^{3+} ions, while Eu^{3+} ions doped into

*Project supported by the National Natural Science Foundation of China (Grant No. 61036001), the Natural Science Foundation of Jiangsu Province, China (Grant No. BK2010010), and the Fundamental Research Funds for the Central Universities of China (Grant Nos. 1112021001 and 1116021003).

†Corresponding author. E-mail: junxu@nju.edu.cn

© 2012 Chinese Physical Society and IOP Publishing Ltd

or co-doped with other nanocrystals showed emission peaks mainly ascribed to the electric dipole transition of Eu^{3+} ions.[15,16]

In this work, a modified sol–gel process is used to obtain nanocrystalline SnO_2 particles with a tetragonal rutile crystalline structure, which is confirmed by transmission electron microscopy (TEM) and X-ray diffraction (XRD) spectra. Due to the effective energy transfer process, the enhanced characteristic emission of Eu^{3+}ions is observed by co-doping with Eu^{3+} ions in sol–gel SiO_2 thin films. We systematically study the influences of the amounts of Sn and the post-annealing temperatures on the photoluminescence characteristics. The emission from Eu^{3+}ions can be enhanced by two orders of magnitude under the optimized parameters. We discuss the different probable locations of Eu^{3+} ions in the sol–gel thin film by comparing the photoluminescence intensity from the magnetic dipole transition of the Eu^{3+} ions with that from the electric dipole transition.

2. Experimental details

SiO_2, Eu^{3+} ions and SnO_2 nanocrystals were chosen as the host material, activator ions and embedded sensitizers, respectively. Tetraethyl orthosilicate and $SnCl_4$ were used to form the SiO_2 matrix and SnO_2 nanocrystals using a modified sol–gel process, as reported in our previous work,[12] while $Eu(NO_3)_3$ was used to form the luminescence center. Distilled water, ethanol and tetraethyl orthosilicate were mixed in a volume ratio of 4:4:2. HCl was dropped into the mixed precursor to adjust the PH value to 2.0, and subsequently, $SnCl_4$ and $Eu(NO_3)_3$ were dissolved into the mixed solution. The amount of Eu^{3+} ions was fixed at 3 mol% and the Sn amounts were changed from 0 to 20 mol%. We measured the Sn atomic concentrations by X-ray photoelectron spectra, and the Sn content in the SiO_2 thin film was 1.37% for the 5 mol% Sn-doped sample, and increased to 3.63% for the 20 mol% doped one. Then the precursor was stirred at 65 °C for 2 h and aged for 24 h. The thin film was fabricated on n-type silicon (100) substrates using the spin coating method, and then annealed at different temperatures.

The film microstructures were characterized by TEM (using a TECHNAI G2 operated at 200 kV). The aged gel was dried at 60 °C for 4 h and milled into powders for the XRD (using 0.1540562 nm Cu $K\alpha$ radiation) test. The samples were also measured by Fourier transform infrared (FT-IR) spectroscopy to investigate the chemical binding configurations. Photoluminescence (PL) and photoluminescence excitation (PLE) spectra (using a Jobin Yvon Fluorolo-3 system under a 30 mW He-Cd laser and a 450 W Xe lamp) were measured to study the excitation and emission processes in a co-doped SiO_2 thin film. A photomultiplier (Hamamatsu 928 PMT) was used as a detector during the PL and PLE tests.

3. Results and discussion

Figure 1 shows the XRD patterns for the corresponding sol–gel SiO_2 powder samples containing 20 mol% Sn and 3 mol% Eu under different annealing conditions. The pattern shows several diffraction peaks assigned to the tetragonal rutile crystalline phase of the SnO_2 crystal (JCPDS NO.41-1445). The crystallization of the samples can be promoted at the high annealing temperature (> 800 °C). There is no other phase of the SnO_2 crystal, even after annealing at high temperature (1000 °C), and the crystallization degree changes little when the annealing time becomes as long as 8 h at 1000 °C. This indicates that SnO_2 nanocrystals with a tetragonal rutile crystalline phase are more stable than other nanocrystals, such as In_2O_3 nanocrystals with a cubic phase[12] and ZnO nanocrystals with a hexagonal phase.[17]

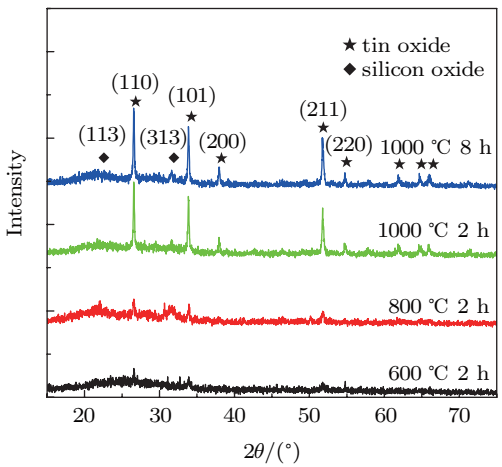


Fig. 1. XRD patterns of the 20 mol% Sn and 3 mol% Eu co-doped SiO_2 powder samples under different annealing conditions.

To further investigate the film microstructures, TEM images of a sol–gel SiO_2 thin film are presented. Figure 2 shows TEM images of SnO_2 and Eu^{3+}ion co-doped thin films after annealing at 1000 °C. Figure 2(a) shows the overview of particles embedded in the

SiO_2 matrix. Crystallized nanoparticles with uniform distribution can be clearly identified in the amorphous SiO_2 matrix. Figure 2(b) shows the rough size distribution of SnO_2 nanocrystals by recording 100 particles. The average size of the particles is around 5 nm after the film is annealed at 1000 °C. Figure 2(c) shows the HRTEM image of the same sample. The interplanar distance is 0.335 nm, corresponding to the (110) lattice spacing of the SnO_2 tetragonal phase.

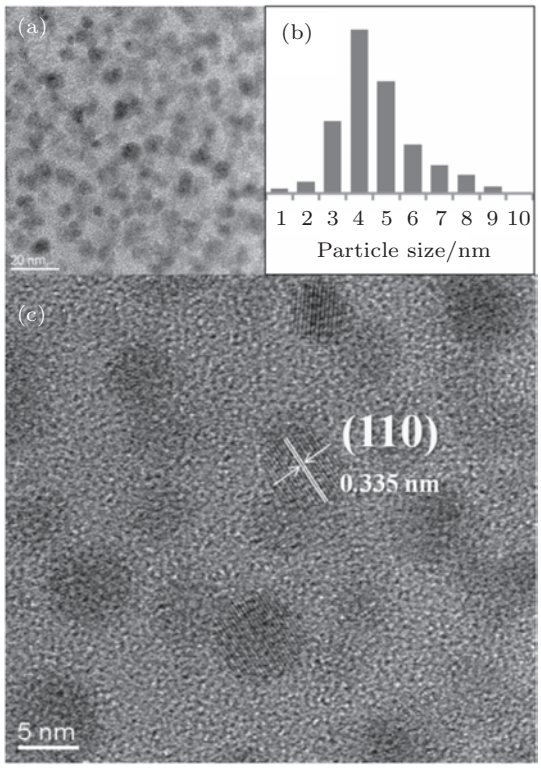


Fig. 2. TEM image of the 20 mol% Sn and 3 mol% Eu co-doped SiO_2 thin film after annealing at 1000 °C. (a) The overview of particles embedded in the SiO_2 matrix, (b) the size distribution of the SnO_2 nanocrystals and (c) the HRTEM of the same sample.

Figure 3 shows the FT-IR spectra of the SiO_2 thin films containing SnO_2 nanocrystals and Eu^{3+} ions after annealing at different temperatures. As can be seen in Fig. 3, the peak centered at 460 cm^{-1} is attributed to the Si–O rocking mode, while the peak centered at 1090 cm^{-1} is attributed to the ASI–TO mode of Si–O–Si. Both the bands centered at 3435 cm^{-1} and 978 cm^{-1} are related to the hydroxyl groups (−OH), which become weaker and weaker with the increasing annealing temperature and finally disappear entirely when the temperature is up to 1000 °C. It was reported that −OH leads to the quenching of the RE emission, which may be the most serious restriction to the luminescence of the RE ion-doped silica materials.[18,19] A post-annealing temperature above 800 °C can effectively enhance the characteristic emission of the RE ions in the sol–gel SiO_2 samples, even without the introduction of a sensitizer, which can be ascribed to the elimination of −OH as indicated by the FT-IR spectra.[12,19] It can be considered that the high temperature above 800 °C is necessary to eliminate the residual −OH.

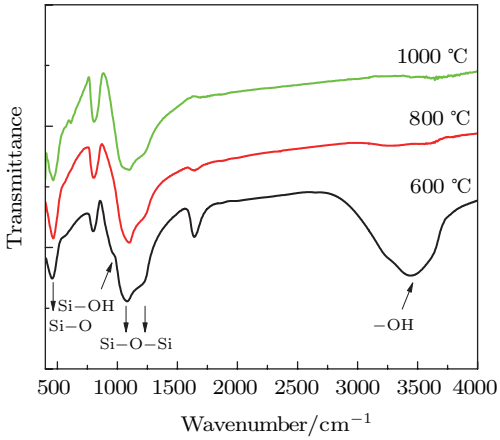


Fig. 3. FT-IR spectra of the 20 mol% Sn and 3 mol% Eu co-doped SiO_2 thin film after annealing at different temperatures.

The room-temperature PL and PLE spectra of SnO_2 nanocrystals without Eu^{3+} ions prepared using different Sn amounts in the SiO_2 host matrix after annealing at 1000 °C are presented in Fig. 4. For PL measurements, the excitation wavelength is kept at 300 nm. After the PL signals are corrected by subtracting the spectral background, a wide band ranging from 400 to 750 nm can be observed and the PL peak center is located at 533 nm. As a comparison, no emission band is detected under the same experimental conditions for the sample without SnO_2, indicating that the green emission band is assigned to the SnO_2 nanocrystals. According to the previous reports,[20–22] the wide PL peak is originated from defect states such as oxygen vacancies and tin interstitials, or dangling on the surface of the SnO_2 nanocrystals. Generally, in the nanocrystalline oxide, oxygen vacancies are well known to be the most common defects and act as radiative centers in the luminescence process. It is found that the high amounts of Sn can enhance the PL intensity because more SnO_2 nanocrystals can be formed. The PLE spectra were measured by keeping the detected wavelength at 533 nm. A sharp excitation band with a maximum at around 300 nm (4.13 eV) is observed, which reveals a wider band-gap for SnO_2 nanocrystals than their bulk counterpart (3.6 eV) owing to the quantum confinement effect. In order to further clarify this point, we

measured the dot size for samples with different Sn concentrations. It is found that the average particle size is increased from 2.9 to 5.3 nm with the increasing Sn amounts (from 5 to 20 mol%). Based on Figs. 4 and 5, as the Sn amounts increase, the PLE peak is slightly red-shifted from 250 to 350 nm, indicating the narrowing of the band gap due to the enlargement of the average particle size.

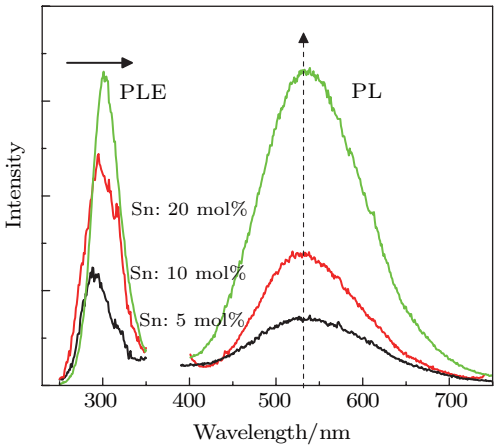


Fig. 4. The PLE spectra of Eu^{3+}-free samples after annealing at 1000 °C by detecting emission at 533 nm, and the PL spectra of the same samples under an excitation wavelength of 300 nm.

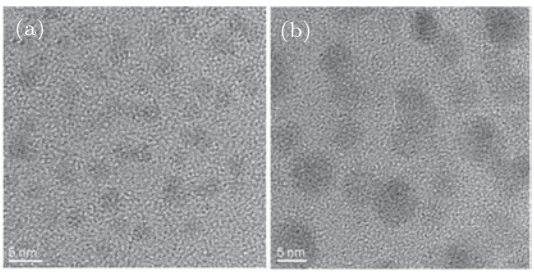


Fig. 5. TEM images of 3 mol% Eu co-doped SiO_2 thin films after annealing at 1000 °C with different Sn amounts: (a) 5 mol% and (b) 20 mol%.

The room-temperature PL spectra of 3 mol% Eu co-doped SiO_2 thin films with different amounts of Sn after annealing at 900 °C for 2 h are presented in Fig. 6. The film without Sn doping shows some weak peaks in red, which can be ascribed to $^5D_0{-}^7F_{j\,(j=0-4)}$ transitions. By Sn co-doping in the film, the SnO_2 nanocrystals can be formed after annealing, as revealed in the XRD and TEM results. Consequently, the characteristic emission from the Eu^{3+} ions is obviously enhanced and the emission intensity of the sample with 20 mol% Sn at 613 nm is enhanced by more than two orders of magnitude compared with that of the sample without Sn co-doping. This phenomenon indicates evidence for the effective energy transfer from the surface defects of SnO_2 nanocrystals to the nearby Eu^{3+} ions. The inset of Fig. 6 shows the changes in the characteristic emission intensity of Eu^{3+} at 613 nm as a function of the Sn doping amounts. This result indicates that co-doping of SnO_2 nanocrystals is an effective way to improve the emission intensity of Eu^{3+} ions.

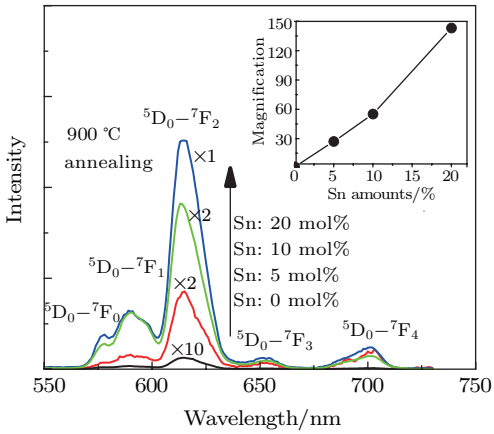


Fig. 6. The room-temperature PL spectra of thin films with 3 mol% Eu co-doped with different amounts of Sn under an excitation wavelength of 300 nm. The inset shows the changes in the characteristic emission intensity of Eu^{3+} ions at 613 nm as a function of the Sn amounts.

In order to further understand the energy transfer process, the PLE spectra of co-doped SiO_2 thin films are carried out by keeping the detected emission wavelength at 613 nm. Figure 7(a) shows the PLE spectra of samples with 20 mol% Sn and 3 mol% Eu amounts after annealing at different temperatures. Several sharp excitation peaks are induced by the 4f–4f transitions of the Eu^{3+} ions. The broad excitation bands of SnO_2 nanocrystals from 250 to 350 nm are red-shifted with the increasing annealing temperatures. This can be explained as the enlargement of the average particle size. Based on the above measurement results, we infer two possible channels for the excitations of the Eu^{3+} ions. The sharp excitation peaks indicate a direct excitation of the Eu^{3+} ions from the ground state to the excited state, while the broad excitation bands indicate an indirect excitation by an energy transfer from SnO_2 nanocrystals to Eu^{3+} ions. We estimated the average size of SnO_2 nanocrystals by using the effective mass theory based on the PLE peak position.[23] The average particle diameter of the SnO_2 nanocrystals after annealing at 1000 °C for 2 h is about 5.0 nm, which is consistent with the TEM observations.

Studying the spectral features of the $^5D_0{-}^7F_{j(0-4)}$ transitions of the Eu^{3+} ions reveals the local environment of the Eu^{3+} ions.[16] Among the $^5D_0{-}^7F_{j(0-4)}$

transitions of the Eu^{3+} ions, the $^5D_0$–$^7F_2$ band is an electric dipole transition which is sensitive to the chemical bonds in the vicinity of Eu^{3+} ions. The $^5D_0$–$^7F_1$ band is a magnetic dipole one and hardly varies with the crystal field strength around the Eu^{3+} ions.[15] We define the fluorescence intensity ratio of the $^5D_0$–$^7F_1$ transition to the $^5D_0$–$^7F_2$ transition as "the symmetry ratio". The symmetry ratio gives an evaluation of the degree of symmetry of the local environment of the Eu^{3+} ions in the matrix. The smaller the value of the symmetry ratio, the weaker the average symmetry of the local environment of the Eu^{3+} ions in the matrix. It is found that the symmetry ratio of the thin films with 3 mol% Eu^{3+} ions and 20 mol% Sn doping after annealing at 800 °C is calculated as 0.193, indicating that the Eu^{3+} ions occupy the low-symmetry sites. It is apparent that the symmetry ratio increases with increasing annealing temperature in Fig. 7(b) and is calculated to be 0.238 for the same sample after annealing at 900 °C, and 1.194 for one after annealing at 1000 °C.

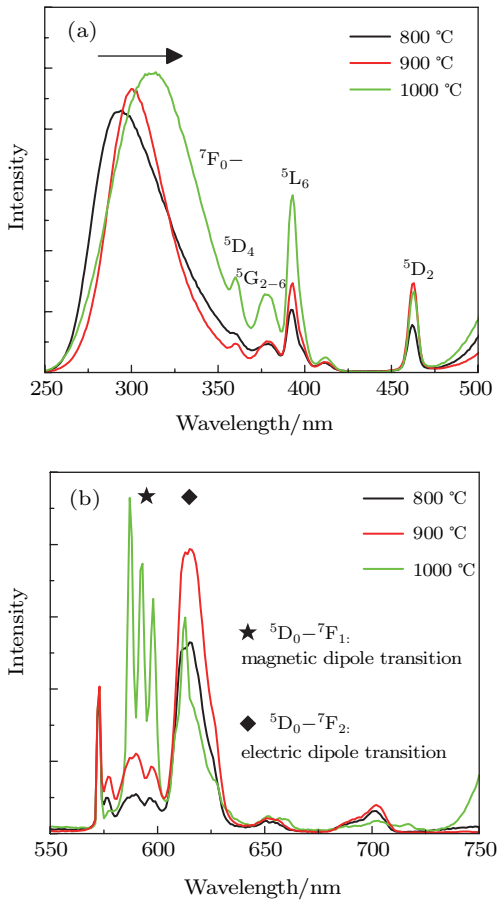


Fig. 7. Room-temperature PL spectra and the PLE spectra of the 3 mol% Eu and 20 mol% Sn co-doped thin film after annealing at different temperatures. (a) PLE spectra of the samples by detecting emission at 613 nm, and (b) PL spectra of the samples under the excitation wavelength of 325 nm.

The SnO_2 exhibits very low solubility for the lanthanide ions (about 0.05%)[24] owing to the difference between the radius of Sn^{4+} (0.076 nm) and that of Eu^{3+} (0.0095 nm). As a consequence, only a low percentage of the Eu^{3+} ions are expected to be partitioned into the SnO_2 nanocrystals by substituting Sn^{4+} at the C_{2h} or D_{2h} sites,[25,26] while most of them would stay in the glassy SiO_2 matrix. In our case, it is apparent that the value of the symmetry ratio increases with the increasing annealing temperature, which may suggest that more Eu^{3+} ions diffuse into the SnO_2 nanocrystals rather than stay in the random glass network structure when the annealing temperature is higher than 800 °C. The increase in the integrated PL intensity indicates that the resonant energy transfer probability from the SnO_2 nanocrystals to the Eu^{3+} ions embedded in them is higher than that to the ones in the glassy SiO_2 matrix. This is because of the shorter average distance between the SnO_2 nanocrystals and the Eu^{3+} ions.

The temperature-dependent PL spectra of co-doped samples annealed at 1000 °C are presented in Fig. 8. The excitation wavelength is kept at 325 nm. The enhancement of emission intensity associated with SnO_2 surface defects and Eu^{3+} ions following the decrease in test temperatures indicates the suppression of the non-radiative process assisted by phonons in the silica matrix. It is also found that the symmetry ratio of Eu^{3+} emission gradually decreases with the decreasing test temperature. At the low test temperature, the emission intensity of the $^5D_0$–$^7F_1$ transition is lower than that of the $^5D_0$–$^7F_2$ transition. It can be explained that the Eu^{3+} ions embedded in the random glass network structures have a much larger probability of releasing their excited energy through phonon-assisted non-radiative recombination than the ones embedded in the crystalline SnO_2. This means that the $^5D_0$–$^7F_2$ emission intensity attributed mainly to the Eu^{3+} ions embedded in the silica matrix is more sensitive to the surrounding temperature than the $^5D_0$–$^7F_1$ emission intensity mainly attributed to the Eu^{3+} ions embedded in the SnO_2 nanocrystals.

According to the room-temperature PL and PLE spectra, the energy transfer process can be described as follows. The UV incident photons (300 nm) are absorbed by SnO_2 nanocrystals. They promote the direct transition of electrons from the valence band to the conduction band. Subsequently, the photoexcited electrons generated by the band-

gap excitation of SnO_2 are trapped by the defect states (oxygen vacancies on the surface of the SnO_2 nanocrystals) via a non-radiative process, and then recombine with the holes in the valence band inducing the 533 nm emission. Finally, this emission energy can be transferred to the nearby Eu^{3+} ions and more electrons will be promoted from the ground state to the excited state, inducing Eu^{3+} ion emission via radiative relaxation. According to the temperature-dependent PL, the enhancement of the emission intensity from the Eu^{3+} ions indicates the suppression of the phonon-assisted non-radiative process with the decrease in test temperature. The non-radiative rate of Eu^{3+} ions declines quicker in silica than in SnO_2 nanocrystals, which induces the increase in the symmetry ratio of Eu^{3+} ion emission with the decrease in test temperatures. With the increasing annealing temperature, Eu^{3+} ions are expected to be partitioned into the SnO_2 nanocrystals by substituting Sn^{4+} at the C_{2h} or D_{2h} sites, inducing the shorter distance between the Eu^{3+} ions and the nanocrystals. The short distance between the Eu^{3+} ions and the nanocrystals is in favor of the high-efficiency emission of the Eu^{3+} ions by the energy transfer.

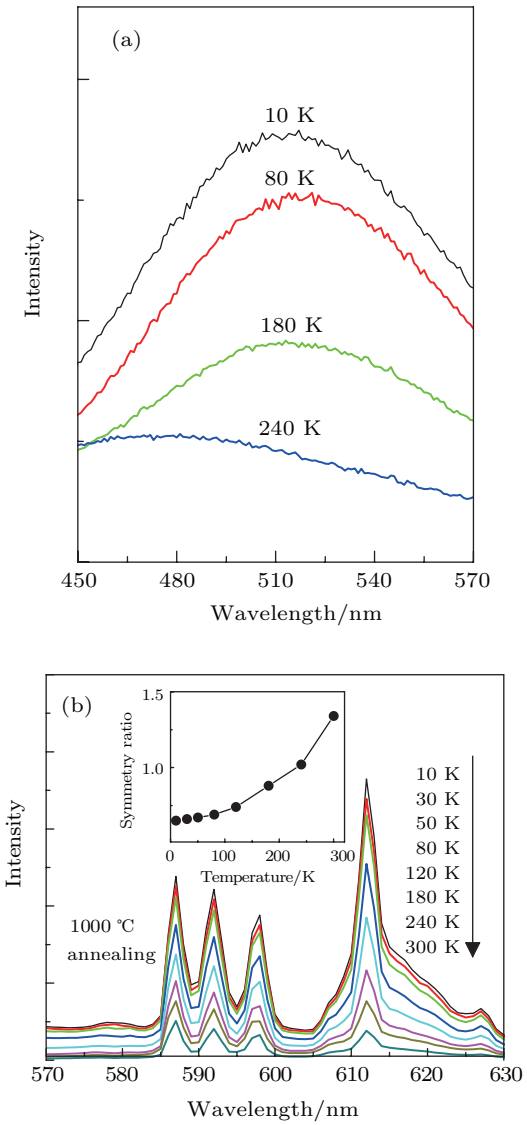


Fig. 8. The temperature-dependent PL spectra of 3 mol% Eu and 20 mol% Sn co-doped thin films after annealing at 1000 °C under a laser excitation wavelength of 325 nm. (a) The emission band ascribed to SnO_2 surface defects, and (b) the characteristic emission peaks of the $^5D_0$–$^7F_{j(1-4)}$ transitions of the Eu^{3+} ions. The inset shows the values of the symmetry ratio with increasing test temperature.

4. Conclusion

In summary, SnO_2 nanocrystals and rare-earth Eu^{3+} ion co-doped SiO_2 thin films were prepared using a sol–gel process. The influences of doping and annealing conditions on the photoluminescence from co-doped films were systematically investigated. The obtained SnO_2 nanocrystals are uniformly distributed with sizes of 4–5 nm. The luminescent intensity of the Eu^{3+} ions is enhanced by more than two orders of magnitude, which can be attributed to the effective energy transfer process due to the formation of SnO_2 nanocrystals of suitable size and density, as well as the elimination of residual −OH in the SiO_2 matrix after 800 °C annealing. Our experimental results indicate that the UV incident photons are absorbed by SnO_2 nanocrystals through band-to-band transition, while the energy transfer process is from oxygen vacancy defects on the surface of SnO_2 nanocrystals to the nearby Eu^{3+} ions. The temperature-dependent PL spectra indicate the diversity of the emission properties assigned to Eu^{3+} ions embedded in the SnO_2 nanocrystals or random silica matrix. The enhancement of the symmetry ratio following the increase in annealing temperature proves the improvement in the diffusion concentration of Eu^{3+} ions in the SnO_2 nanocrystals and the energy transfer efficiency.

References

[1] Najar A, Charrier J, Lorrain N and Haji L 2007 *Appl. Phys. Lett.* **91** 121120

[2] Li P L, Yang Z P, Wang Z J and Guo Q L 2008 *Chin. Phys.* B **17** 1135

[3] Lourenço M A, Gwilliam R M and Homewood K P 2007 *Appl. Phys. Lett.* **91** 141122

[4] Otona C J, Loh W H and Kenyon A J 2006 *Appl. Phys. Lett.* **89** 031116
[5] Lockwood D J and Pavesi L 2004 *Top. Appl. Phys.* **94** 1
[6] Shin J H, Hoven G N V and Polman A 1995 *Appl. Phys. Lett.* **66** 2379
[7] Fujii M, Yoshida M, Kanzawa Y, Hayashi S and Yamamoto K 1997 *Appl. Phys. Lett.* **71** 1198
[8] Timoshenko V Y, Lisachenko M G, Shalygina O A, Kamenev B V, Zhigunov D M, Teterukov S A and Kashkarov P K 2004 *J. Appl. Phys.* **96** 2254
[9] Vinh N Q, Minissale S, Andreev B A and Gregorhkevica T 2003 *J. Phys.Condens. Matter* **17** S2191
[10] Zeng X Y, Yuan J L, Wang Z Y and Zhang L D 2007 *Adv. Mater.* **19** 4510
[11] Li X, Zhai F F, Liu Y, Cao M S, Wang F C and Zhang X X 2007 *Chin. Phys.* B **16** 2769
[12] Lin T, Ding X Y, Xu J, Wan N, Xu L and Chen K J 2011 *J. Appl. Phys.* **109** 083512
[13] Yu Y L, Chen D Q, Wang Y S, Huang P, Weng F Y and Niu M T 2009 *Phys. Chem. Chem. Phys.* **11** 8774
[14] Wan N, Lin T, Xu J, Xu L and Chen K J 2008 *Nanotechnology* **19** 095709
[15] Nogami M, Enomoto T and Hayakawa T 2002 *J. Lumin.* **97** 147
[16] Yu Y L, Chen D Q, Huang P, Lin H, Yang A P and Wang Y S 2011 *Journal of Solid State Chemistry* **184** 236
[17] Fang Z B, Tan Y S, Liu X Q, Yang Y H and Wang Y Y 2004 *Chin. Phys.* **13** 1330
[18] Biswas A, Maciel G S, Kapoor R, Friend C S and Prasad P N 2003 *Appl. Phys. Lett.* **82** 2389
[19] Fukushima M, Managaki N, Fujii M, Yanagi H and Hayashi S 2005 *J. Appl. Phys.* **98** 024316
[20] Zhou J X, Zhang M S and Hong J M 2005 *Appl. Phys.* A **81** 177
[21] Gu F, Wang S F and Song C F 2003 *Chem. Phys. Lett.* **372** 451
[22] Lin T, Wan N, Han M, Xu J and Chen K J 2009 *Acta Phys. Sin.* **58** 5821 (in Chinese).
[23] Brus L 1986 *J. Phys. Chem.* **90** 2555
[24] Morais E A, Ribeiro S J L, Scalvi L V A, Santilli C V, Ruggiero L O, Pulcinelli S H and Messaddeq Y 2002 *J. Alloy Compd.* **344** 217
[25] Chen J, Wang J, Zhang F, Yan D, Zhang G, Zhuo R and Yan P 2008 *J. Phys.* D **41** 105306
[26] Moon T, Hwang S T, Jung D R, Son D, Kim C, Kang M and Park B 2007 *J. Phys. Chem.* C **111** 4164